

# Technical Notes

*TECHNICAL NOTES* are short manuscripts describing new developments or important results of a preliminary nature. These Notes cannot exceed six manuscript pages and three figures; a page of text may be substituted for a figure and vice versa. After informal review by the editors, they may be published within a few months of the date of receipt. Style requirements are the same as for regular contributions (see inside back cover).

## Damage Identification of Plate Structures Using a Hybrid Genetic-Sensitivity Approach

Scott M. Bland\* and Rakesh K. Kapania†  
Virginia Polytechnic Institute and State University,  
Blacksburg, Virginia 24061

### Introduction

INTEREST in global structural health monitoring has grown rapidly as the number of aging structures in service increases. Structural health monitoring offers the possibility of detecting and identifying structural damage before catastrophic failure occurs. Currently, vibration-based damage detection and identification techniques offer the greatest promise for future development of an operational global structural health monitoring system. One method for vibration-based damage identification presented by Mares and Surace<sup>1</sup> used a genetic algorithm (GA) to select parameters in a finite element model of the structure so that the differences between the experimental and calculated dynamic properties were minimized. Differences between the calculated model parameters and some baseline set of model parameters for the undamaged structure indicated damage. Friswell et al.<sup>2</sup> used a combined genetic and eigensensitivity algorithm in order to incorporate the search capabilities of the GA and the efficiency of sensitivity techniques. This hybrid method offers the search capabilities of the GA and the efficiency of sensitivity methods.

This work further examines the effectiveness of a hybrid-genetic-sensitivity (HGS) approach<sup>3</sup> for damage identification for stiffened plate structures using changes in the natural frequencies and mode shapes between the damaged and undamaged structure. Three cases were examined for a uniaxially stiffened clamped plate (USCP) and cross-stiffened clamped-plate (CSCP) structures: one damage site case, one damage site with 5% white noise added to the calculated modal parameters, and two damage site case.

### Hybrid-Genetic-Sensitivity Approach for Damage Identification

#### Damage Identification Problem

The damage identification problem in this study is posed as an optimization problem: to minimize the difference between the exper-

imental modal parameters of the damaged structure and the modal parameters of the structure found using a finite element model of the structure. This assumes that a correlated finite element model of the undamaged structure exists. The plate structures considered here are isotropic, and damage is modeled by reductions in the elastic modulus  $E$  and Poisson's ratio  $\nu$  of a particular finite element. The design variables in the damage identification optimization problem were the ratios of the elastic modulus and Poisson's ratio of the damaged element(s) to the undamaged values.

The objective function for the damage identification problem is shown in Eq. (1). This objective function is used for the general damage case, where all of the elements in the finite element model could feasibly be damaged simultaneously. The third term in Eq. (1) is used to reduce the "smearing" of parameter changes over many elements because damage, especially at the incipient stages, is usually a local phenomenon:

$$f(\omega, \phi, N_{\text{elem}}) = \alpha \sum_{r=1}^n \left( \frac{\omega_{\text{exp}}^r - \omega_{\text{mod}}^r}{\omega_{\text{mod}}^r} \right)^2 + \beta \sum_{r=1}^n \sum_{i=1}^{n_{\text{dof}}} \left( \frac{\phi_{\text{exp}}^{ri} - \phi_{\text{mod}}^{ri}}{\phi_{\text{mod}}^{ri}} \right)^2 + \gamma \left( \frac{N_{\text{dam}}}{N_{\text{total}}} \right) \quad (1)$$

In this equation  $\omega_{\text{exp}}^r$  and  $\omega_{\text{mod}}^r$  are the  $r$ th experimental and modeled natural frequencies of the structure,  $\phi_{\text{exp}}^{ri}$  and  $\phi_{\text{mod}}^{ri}$  are the  $r$ th experimental and modeled mode shapes of the structure,  $N_{\text{dam}}$  is the number of damaged elements, and  $N_{\text{total}}$  is the number of elements in the finite element model. The variables  $\alpha$ ,  $\beta$ , and  $\gamma$  are the weighting coefficients of the terms in the objective function.

The values of the weighting coefficients  $\alpha$ ,  $\beta$ , and  $\gamma$  were determined using trial and error because no widely accepted means of determining these values is available. Two versions of the objective function were used in this study. The first version considered only one possible damage site, and so  $\gamma$  was set to zero in Eq. (1). In this case the weighting coefficients used were chosen such that the natural frequency information accounted for 80% of the objective function value and the mode shape information accounted for 20%. These weighting coefficients ensured that more importance was given to the natural frequency information, which can be measured with higher accuracy. In the general damage case, where an arbitrary number of damage sites can exist,  $\gamma$  in Eq. (1) was nonzero. The best combination of weightings in the general damage case was found when the natural frequency information accounted for 60%, mode-shape information accounted for 20%, and the number of damage sites accounted for 20% of the total objective function value. The actual values of the weighting coefficients were unique for each case because the number of elements and degrees of freedom for various cases could be different.

#### Hybrid-Genetic-Sensitivity Method

An elitist selection scheme was used for the GA in this study, which ensured that the best individual in every population was held over to the next generation. A crossover rate of 0.9 and a mutation rate of 0.1 were used in the GA portion of the HGS approach to ensure that the design space was highly explored. The high crossover and mutation rates are essential in this application for increased exploration of the design space. The high crossover and mutation rates tend to slow the convergence to the optimal values by the GA, but

Presented as Paper 2002-5463 at the AIAA/ISSMO 9th Symposium on Multidisciplinary Analysis and Optimization, Atlanta, GA, 4–6 September 2002; received 17 July 2003; revision received 13 September 2004; accepted for publication 14 September 2004. Copyright © 2004 by the American Institute of Aeronautics and Astronautics, Inc. All rights reserved. Copies of this paper may be made for personal or internal use, on condition that the copier pay the \$10.00 per-copy fee to the Copyright Clearance Center, Inc., 222 Rosewood Drive, Danvers, MA 01923; include the code 0001-1452/05 \$10.00 in correspondence with the CCC.

\*Graduate Research Assistant, Department of Aerospace and Ocean Engineering, Student Member AIAA.

†Professor, Department of Aerospace and Ocean Engineering, Associate Fellow AIAA.

this was not a major concern because a sensitivity-based procedure was used later to refine the best individuals in the final population.

To ensure that the best starting points were selected by the GA, while reducing the computational cost, a relatively large population size was used over a relatively few generations. In this study the population size was set at 20 individuals, and the GA was run over 20 generations. The GA reduces the average objective function value quickly over the first 10 generations, and then the average objective function value of the population stagnates because the GA is not efficient at refining the design points. For this reason, the GA is stopped at 20 generations, and a sensitivity-based optimization is then used to complete the optimization process. Usually, the final population of the GA will have many individuals with design points that are very close to each other; these individuals usually correspond to the optimum design in different stages of refinement. The individuals selected to be refined by the sensitivity-based optimization had to be sufficiently far apart from each other in the design space. To discriminate between two individuals representing the same element in the final population, Eq. (2) was used to find the distance between the designs:

$$d_{i,j} = \sqrt{(E_i - E_j)^2 + (v_i - v_j)^2} \quad (2)$$

where  $d_{i,j}$  is the distance between the  $i$ th and the  $j$ th individuals in the final population,  $E_i$  and  $E_j$  are the elastic modulus of the  $i$ th and the  $j$ th individuals, and  $v_i$  and  $v_j$  are the Poisson's ratio of the  $i$ th and the  $j$ th individuals. If the value of  $d_{i,j}$  was less than 0.001, the  $j$ th individual is not used in the sensitivity-based optimization because it is sufficiently close to the  $i$ th individual. If all of the individuals in the population are sufficiently close to each other in the design space, only one value is selected for refinement. The "fmincon" routine in the Optimization Toolbox for MATLAB<sup>®</sup>,<sup>4</sup> which is a nonlinear optimization routine, was used with the stopping criteria defined as  $\Delta f < 0.0001$  or a maximum of 20 iterations.

### Performance of the HGS Method on Plate Examples

The performance of the HGS method for damage identification is demonstrated here for a uniaxially stiffened clamped plate and a cross-stiffened clamped plate using numerical examples. Both plates were clamped on all four sides of the plate. Figure 1 shows the geometry of the plate model used in the study. The stiffener in the plate was made of the same material as the rest of the plate and was modeled using beam elements in the SDT Toolbox for MATLAB.<sup>5</sup> The thickness of the stiffeners was 10 mm in both cases.

The geometric properties of the plates denoted in Fig. 1 were  $W = 0.3$  m,  $L = 0.357$  m, and  $t = 0.01$  m. The material properties of the undamaged plate examples were density  $\rho = 2770$  kg/m<sup>3</sup>; elastic modulus  $E = 7.31 \times 10^4$  MPa; and Poisson's ratio  $\nu = 0.33$ .

The first scenario analyzed using the HGS approach was one damage site using the objective function in given in Eq. (1) with  $\gamma = 0$  for both the USCP and CSCP. The plate for both the USCP and CSCP was modeled using an  $8 \times 8$  four-noded finite element model from the SDT Toolbox.<sup>5</sup> Figure 2 shows the performance of the HGS

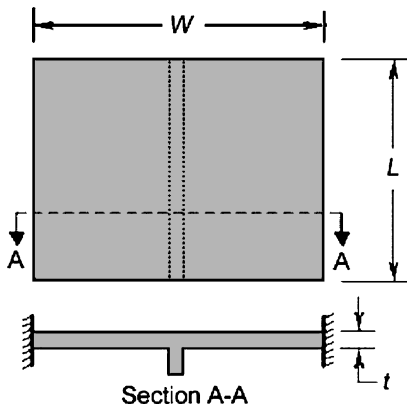


Fig. 1 Layout of the uniaxially stiffened clamped plate example.

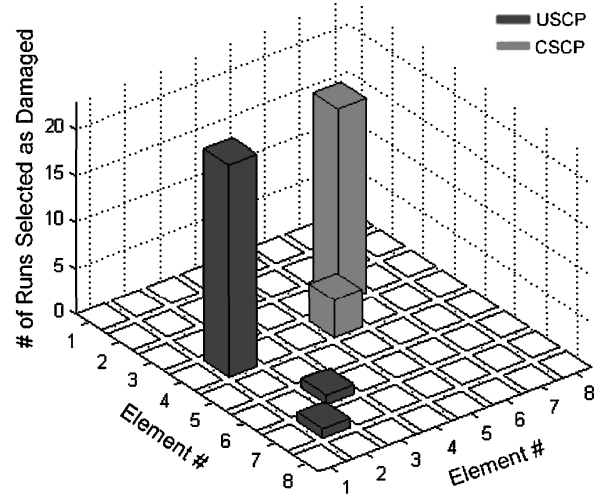


Fig. 2 Damage locations found by the HGS algorithm for USCP and CSCP using an  $8 \times 8$  mesh and one damage site.

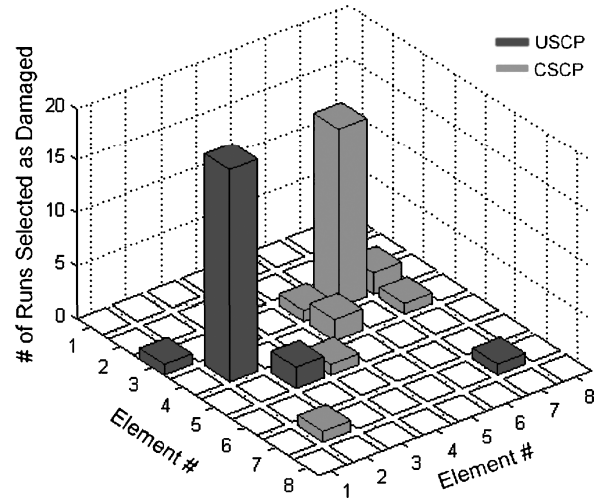


Fig. 3 Damage locations found by the HGS algorithm for the USCP and CSCP using an  $8 \times 8$  mesh with 5% white noise in the simulated experimental data for one damage site.

approach in finding the single damage location for both the USCP and CSCP over 25 runs. In this figure the  $8 \times 8$  grid represents the finite element mesh of the plate, and the columns indicate the number of times the corresponding element was selected as the damaged element by the HGS algorithm. The damaged element for the USCP is element (4, 2), and the damaged element for the CSCP is element (3, 6). The HGS algorithm found the correct damage location 23 of 25 runs for the USCP case and 21 of 25 runs for the CSCP case.

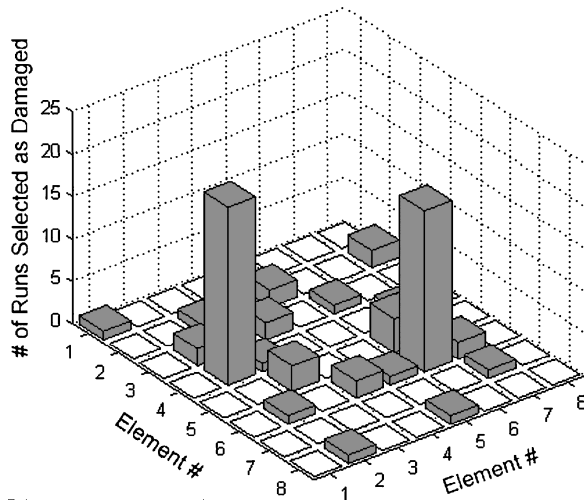
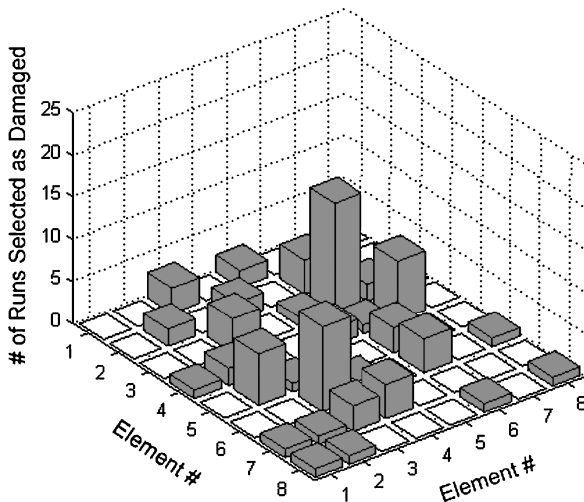
To examine the robustness of the HGS algorithm, 5% white noise was added to the calculated modal parameters to simulate experimental signal noise for the single damage site case. Again, the objective function given in Eq. (1) with  $\gamma = 0$  was used for both the USCP and CSCP, and an  $8 \times 8$  finite element mesh was used for the plate. The performance of the HGS approach in finding the single damage location with added 5% white noise for both the USCP and CSCP over 25 runs is shown in Fig. 3. The damage sites were the same for this case as in the single damage site case just cited. The correct damaged element was determined 20 out of 25 runs for the USCP case and 17 out of 25 runs for the CSCP case.

The performance of the HGS approach in identifying the material properties at the damage location is shown in Table 1 for both the single damage site case and the single damage site with added random noise case.

The next case examined was for two damage locations on the USCP and CSCP examples. Figure 4 shows the results of the HGS approach for two damage sites on the USCP example using the

**Table 1** Comparison of percent relative error in the results obtained from a pure GA algorithm and the HGS approach various example cases

Case	$E$ (GA)	$\nu$ (GA)	$E$ (HGS)	$\nu$ (HGS)
USCP(1)	6.098	9.434	3.235	7.334
USCP(2)	8.987	15.54	4.26	8.83
CSCP(1)	13.06	24.43	12.75	18.83
CSCP(2)	7.830	9.484	4.023	7.234
CSCP(1)	15.30	25.03	10.47	17.32
CSCP(2)	43.76	56.98	32.67	38.92

**Fig. 4** Damage locations found by the HGS algorithm for a USCP using an  $8 \times 8$  mesh with two damage sites.**Fig. 5** Damage locations found by the HGS algorithm for a CSCP with an  $8 \times 8$  mesh with two damage sites.

objective function in Eq. (1) with  $\gamma \neq 0$  over 25 runs. The damage locations were in the positions (4, 2) and (6, 6) on the mesh.

The HGS approach correctly found the damage sites the majority of the time; the number of erroneous damage sites selected increased over the single damage site cases. The HGS approach found the correct damage location (4, 2) in 21 of the 25 runs, whereas the correct damage location at the (6, 6) position was found in 18 of the 25 runs. Because an arbitrary number of damage sites were feasible, some of the damage detected by the HGS approach was smeared over other elements to try to match the experimental data. Figure 5 shows the damage locations found by the HGS approach for the CSCP example with two damage sites. This figure shows that the HGS algorithm

finds the damage in location (6, 3) in 13 of the 25 runs and in location (3, 6) in 15 of the 25 cases. The accuracy of the damage location for this case was lower than any of the other cases. This could be caused by the cross stiffeners that reduce the effects of the damage on the modal properties. This case shows that an objective function that allows an arbitrary number of damage locations might not be the best option because the damage is again smeared over many elements.

Table 1 shows a comparison of the HGS approach to the GA-only approach for the three cases just mentioned using the USCP and CSCP examples. Both the GA and the HGS approach were limited to 420 objective function evaluations. The case labeled USCP(1) and CSCP(1) represent the uniaxially stiffened clamped plate and cross-stiffened plate example with one damage site. The cases denoted USCP(2) and CSCP(2) represent the case with two damage sites. The results in this table correspond to the damage locations described for each of the cases in the preceding sections and are averaged over the 25 runs.

The results in Table 1 show that again the HGS algorithm has superior performance compared to the pure GA damage identification algorithm for both the USCP and CSCP cases. Most of the improvements made by the HGS algorithm were in refining the values of the damage parameters again. The accuracy of the both GA and HGS approach for the two damage site case is relatively low, and a different method would probably be required to find damage in this case and damage in those locations. But in general the HGS approach gives significant improvement over a pure GA damage identification algorithm.

## Conclusions

The hybrid-genetic-sensitivity (HGS) approach was demonstrated for two plate structures: a uniaxially stiffened clamped plate and a cross-stiffened clamped plate. The HGS approach was shown in all cases to outperform a pure genetic-algorithm (GA)-based algorithm using the same number of objective function evaluations. The HGS approach was also shown to be robust with reasonable performance when white noise was included in the simulated experimental data. These results show that it is possible to solve damage identification problems more efficiently using a combination of optimization procedures by utilizing the positive attributes of each component of the algorithm. In this case the exploration characteristics of GAs were exploited to find starting points for a sensitivity-based optimization procedure, which is much more efficient in refining results. This combination resulted in global optimization with improved efficiency over a pure GA.

## References

- Mares, C., and Surace, C., "An Application of Genetic Algorithms to Identify Damage in Elastic Structures," *Journal of Sound and Vibration*, Vol. 195, No. 2, 1996, pp. 195–215.
- Friswell, M. I., Penny, J. E. T., and Garvey, S. D., "A Combined Genetic and Eigensensitivity Algorithm for the Location of Damage in Structures," *Computers and Structures*, Vol. 69, No. 5, 1998, pp. 547–556.
- Bland, S. M., and Kapania, R. K., "Damage Detection Using a Hybrid Genetic Sensitivity Approach," *Advances in Computational Engineering and Sciences, Proceedings of the 2002 International Conference on Computational Engineering and Sciences (ICES'02)*, edited by S. N. Atluri and D. W. Pepper, Tech Science Press, Forsyth, GA, 2002.
- "Optimization Toolbox User's Guide," MathWorks, Inc., Natick, MA, 2002, URL: [http://www.mathworks.com/access/helpdesk/help/pdf\\_doc/optim/optim\\_tb.pdf](http://www.mathworks.com/access/helpdesk/help/pdf_doc/optim/optim_tb.pdf) [cited 1 June 2003].
- Balmes, E., and Leclerc, J. M., "Structural Dynamics Toolbox User's Guide," SDTools, Paris, 2002, URL: <http://www.sdtools.com/pdf/sdt.pdf> [cited 1 June 2003].

E. Livne  
Associate Editor